

Biliary Infections: Spectrum of Imaging Findings and Management¹

CME FEATURE

See accompanying test at http://www.rsna.org/education/rg_cme.html

LEARNING OBJECTIVES FOR TEST 4

After reading this article and taking the test, the reader will be able to:

- Describe the spectrum of biliary infections affecting immunocompetent and immunocompromised patients.
- List the key clinical and imaging features of cholangitis.
- Discuss the current treatment of cholangitis, including the role of ERCP and PTC.

TEACHING POINTS

See last page

Onofrio A. Catalano, MD • Dushyant V. Sahani, MD • David G. Forcione, MD • Benedikt Czermak, MD • Chang-Hsien Liu, MD • Andrea Soricelli, MD • Ronald S. Arellano, MD • Peter R. Mueller, MD • Peter F. Hahn, MD, PhD

Infectious cholangitides encompass a wide spectrum of infectious processes affecting the biliary tree. They can have protean clinical and imaging appearances. Some manifest as an acute medical emergency with high mortality if not properly and emergently managed. Others are chronic processes that may predispose a patient to liver failure or cholangiocarcinoma. The clinical and imaging features and the subsequent therapy are dictated by the pathogens involved, the immune status of the host, and the degree and distribution of biliary obstruction. Bacteria cause most cases of infectious cholangitis in Western countries. In other parts of the world, parasites play an important role, either as causative agents or in predisposing the host to bacterial superinfection. Viral cholangitides primarily affect immunocompromised patients. The clinical and imaging features of cholangitis differ between immunocompetent and immunocompromised patients. Imaging plays a pivotal role in diagnosis of infectious cholangitis, helps identify predisposing causes, and demonstrates complications. Moreover, interventional radiology provides tools to treat acute life-threatening biliary infections, chronic entities, and complications.

©RSNA, 2009 • radiographics.rsna.org

Abbreviations: BAC = bacterial acute cholangitis, CBD = common bile duct, ERCP = endoscopic retrograde cholangiopancreatography, HIV = human immunodeficiency virus, OLT = orthotopic liver transplantation, PTC = percutaneous transhepatic cholangiography, RPC = recurrent pyogenic cholangitis

RadioGraphics 2009; 29:2059–2080 • **Published online** 10.1148/rg.297095051 • **Content Codes:** **GI** **VI**

¹From the Departments of Radiology (O.A.C., D.V.S., R.S.A., P.R.M., P.F.H.) and Gastroenterology (D.G.F.), Harvard Medical School and Massachusetts General Hospital, 55 Fruit St, Boston, MA 02114; the Department of Radiology, Medical School, University of Innsbruck, Innsbruck, Austria (B.C.); the Department of Radiology, Tri-Service General Hospital and National Defense Medical Center, Taipei, Taiwan (C.H.L.); and the Department of Radiology, University of Naples Parthenope and SDN Foundation-IRCCS, Naples, Italy (A.S.). Recipient of a Certificate of Merit award for an education exhibit at the 2008 RSNA Annual Meeting. Received March 16, 2009; revision requested April 27; final revision received July 13; accepted July 15. D.V.S. receives research support from General Electric; all other authors have no financial relationships to disclose. **Address correspondence to** O.A.C. (e-mail: ocatalano@partners.org).

Introduction

The terms *biliary infections* and *infectious cholangitides* are used to indicate infectious processes affecting the biliary tree, regardless of the infectious agents and of the clinical and imaging presentations. They can manifest acutely, in some cases as medical emergencies, or more indolently. The clinical and imaging features and the subsequent therapy are dictated by the pathogens involved, the immune status of the host, and the degree and distribution of biliary obstruction.

Bacteria cause most cases of infectious cholangitis in Western countries. In other parts of the world, parasites play an important role, either as causative agents or in predisposing the host to bacterial superinfection. Viral cholangitides primarily affect immunocompromised patients. Clinical and imaging features of cholangitis differ between immunocompetent and immunocompromised patients. Therefore, cholangitis in immunocompetent patients and cholangitis in immunocompromised patients are treated separately in this article.

Cholangitis in Immunocompetent Patients

Bacterial Acute Cholangitis

Bacterial acute cholangitis (BAC) is a potentially life-threatening disease induced by acute biliary infection, usually in the setting of obstruction (1). The Charcot triad refers to the clinical symptoms of fever, pain, and jaundice. When shock and lethargy are included in this clinical scenario, it is referred to as the Reynolds pentad (2).

Development of BAC requires biliary bacterial contamination, stagnant bile, and increased intrabiliary pressure (≥ 20 cm H₂O) (2–4).

Bile is usually sterile fluid. This is due to a number of factors, including continuous antegrade bile flow toward the duodenum, protective effect of the sphincter of Oddi, bacteriostatic biliary salts, and secretory immunoglobulin A (IgA) of the bile. Moreover, the bacterial burden of the proximal jejunum and duodenum is low, at least in part due to the biliary salts and IgA that flow into the duodenum through the bile (2).

Mortality (3.5%–65%) and severity of acute cholangitis have been shown to correlate with intrabiliary pressure (2–4). Elevated biliary pressure increases permeability of biliary ductules,

thus allowing bacteria and their toxins entry into the bloodstream. Elevated biliary pressure also interferes with intrabiliary secretion of IgA, which in turn reduces the antibacterial properties of the bile. This ultimately results in increased amounts of duodenal and jejunal bacteria. Partial biliary obstruction, which interferes with the biliary protective mechanisms but permits unimpeded access by bacteria to the biliary tree, is associated with higher rates of positive biliary cultures than is complete biliary obstruction. Bile cultures are positive in 50% of patients with choledocholithiasis (2,3).

Obstruction of the common bile duct (CBD) by stones is still the most frequent cause of BAC, with acute cholangitis occurring in 6%–9% of patients admitted for gallstone disease. Choledocholithiasis accounts for up to 80% of cases of acute cholangitis (4).

In recent years, the prevalence of other causes of BAC, including instrumentation of the biliary tree, malignant disease, and sclerosing cholangitis, has increased. Malignancies currently account for 10%–30% of all the cases (3,5).

Advanced age (>70 years), neurologic disease, and periampullary diverticula are risk factors for development of cholangitis in patients with biliary stones (6).

Biliary cultures are polymicrobial in 30%–80% of patients; gram-negative rods are found in 88% of these cases (7,8).

BAC can be a life-threatening emergency if not recognized and treated promptly. Clinical diagnosis is challenging, since the classic Charcot triad occurs in fewer than 75% of patients and blood cultures are positive in only 20%–30% (2,9).

The classic clinical symptoms are often absent or more difficult to recognize in elderly patients, leading to delayed diagnosis or even misdiagnosis. This subset of patients also frequently has comorbidities that increase the severity of cholangitis (6,10).

Acute complications of BAC include sepsis, hepatic abscesses, portal vein thrombosis, and bile peritonitis. Chronic BAC can result in portal vein thrombosis, biliary stricture, sclerosing cholangitis, and cholangiocarcinoma. Both portal vein thrombosis and hepatic abscesses can be clinically silent and detected only with imaging (2,11).

Diagnostic imaging of cholangitis is necessary to assess BAC-associated biliary changes (Figs 1, 2) and parenchymal changes (Figs 3–5).

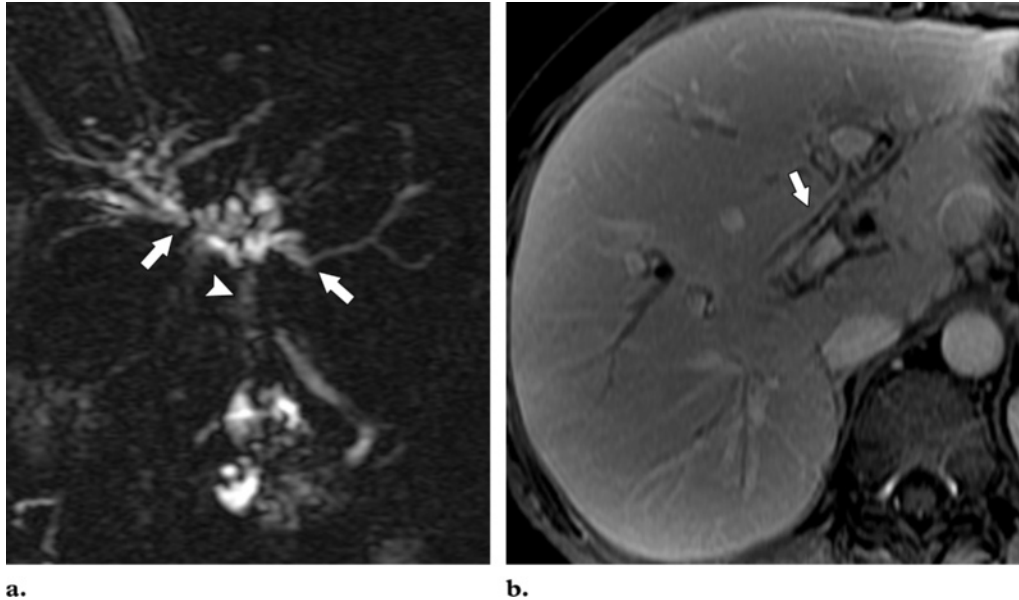


Figure 1. Bile duct changes in BAC. **(a)** Coronal oblique image from T2-weighted magnetic resonance (MR) cholangiopancreatography shows that the intrahepatic biliary ducts are dilated (arrows) because of a stricture (arrowhead) caused by an extrahepatic cholangiocarcinoma. **(b)** Axial gadolinium-enhanced fat-saturated T1-weighted MR image shows inflamed intrahepatic bile duct walls (arrow) that are mildly and symmetrically thickened and enhance with gadolinium.



Figure 2. BAC in a patient with CBD stones. Coronal image from contrast material-enhanced multidetector computed tomography (CT) shows pus (arrowhead) layering within one of several dilated intrahepatic ducts (arrows). Intraductal sludge could have the same appearance. The patient underwent biliary drainage; abundant pus was aspirated.

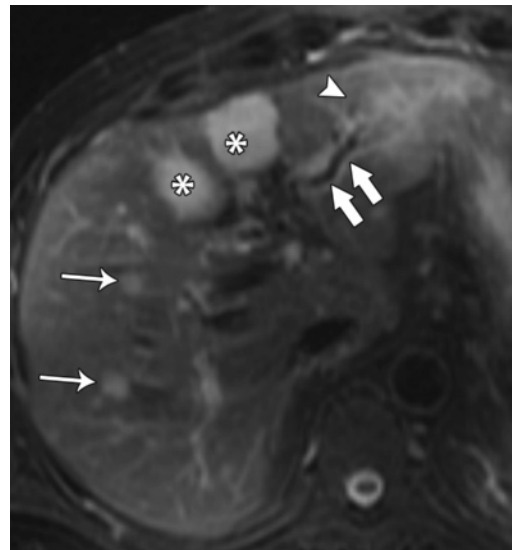


Figure 3. Parenchymal changes in BAC. Axial fat-saturated T2-weighted MR image shows cholangitis as both patchy (thin arrows) and wedge-shaped (arrowhead) areas of increased parenchymal signal intensity. There are inflamed dilated intrahepatic bile ducts with pneumobilia (thick arrows). * = incidental hemangiomas.

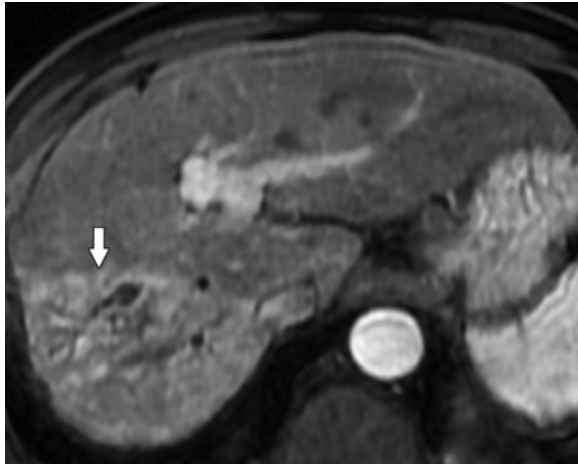


Figure 4. Parenchymal changes in BAC. Axial fat-saturated T1-weighted MR image shows segmental parenchymal enhancement (arrow).

The CBD exhibits diffuse and concentric wall thickening and enhancement in the majority of patients (12).

To our knowledge, there are no dedicated studies on dilatation of extrahepatic biliary ducts in BAC. However, because the majority of cases are associated with choledocholithiasis-induced obstruction of the distal CBD, CBD dilatation is an expected finding.

Dilatation of intrahepatic biliary ducts occurs in all cases. The distribution can be central (38% of cases), diffuse (16%), or segmental (46%). In 85% of the cases, there is associated wall thickening that is smooth and symmetric (13). Pneumobilia can also be present in cases of BAC.

Enhancement of intrahepatic biliary duct walls is a common finding, reported in up to 92% of cases investigated with MR imaging. It is best seen with gadolinium-enhanced delayed phase fat-suppressed sequences (13).

Parenchymal changes seen at imaging in BAC are likely related to extension of the inflammatory process into the periportal tissues and surrounding liver, as well as to dilatation of the peribiliary venous plexus and to increased arterial flow (13,14).

Parenchymal changes include increased signal intensity on T2-weighted images (69%), which can have a wedge-shaped or peribiliary distribution. Hepatic contrast enhancement can be arterial only (58%), delayed only (16%), or arterial

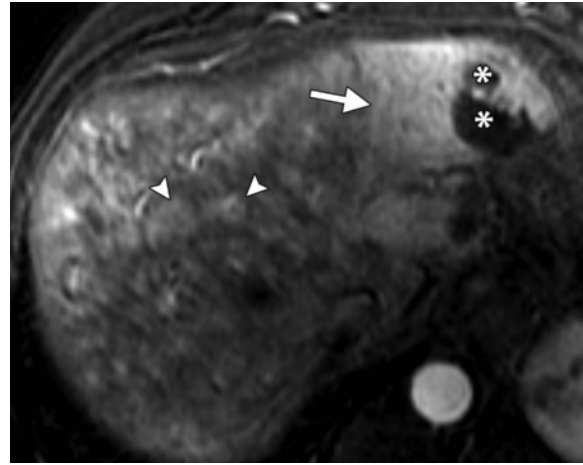


Figure 5. Parenchymal changes in BAC. Axial gadolinium-enhanced fat-saturated T1-weighted MR image shows inflammation as areas of markedly increased parenchymal enhancement in a peribiliary (arrowheads) and wedge-shaped (arrow) distribution. * = abscesses.

and delayed (26%). Patterns of enhancement can be wedge-shaped (72%), peripheral patchy (14%), or peribiliary (14%) in distribution (13).

Other signs of BAC are related to its complications and include liver abscesses (24%) (Fig 6) and portal vein thrombosis (16%) (Fig 7) (13).

Some imaging findings show correlation with the clinical severity of the disease. In particular, marked inhomogeneous parenchymal enhancement in the arterial dominant phase of imaging has been found more often in patients with acute suppurative cholangitis (60% of the cases), which is characterized by the presence of pus in the biliary tree. Moreover, an intensely enhancing, enlarged (>10 mm), and bulging papilla has a high sensitivity (60%) and specificity (86%) for suppurative cholangitis (15).

Cross-sectional imaging also helps assess for the underlying condition responsible for BAC, such as biliary stones, strictures, or neoplasms (2,9,13,16).

To our knowledge, there are no specific studies comparing multidetector CT with MR imaging in the setting of BAC. However, it is our opinion that MR imaging would be more helpful than multidetector CT because of the higher signal-to-noise and contrast-to-noise ratios. A typical MR imaging protocol could include the following sequences: coronal oblique T2-weighted MR cholangiopancreatography, axial T1-weighted in-phase and out-of-phase imaging, axial fat-saturated T2-weighted

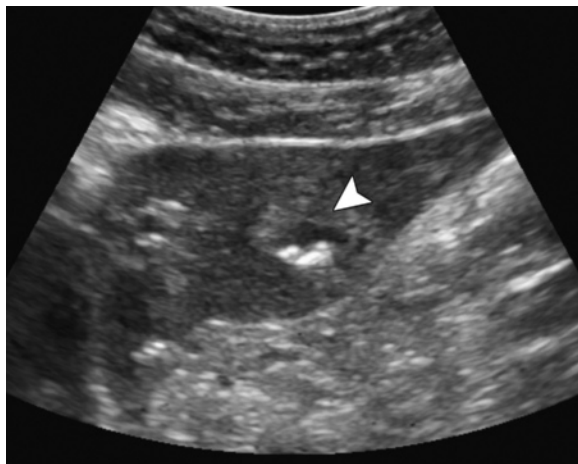
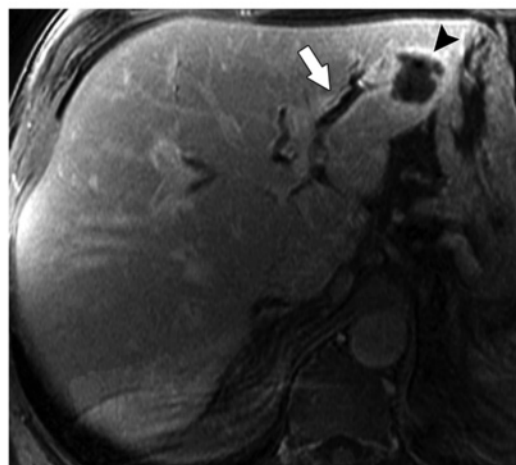


Figure 6. Liver abscesses complicating BAC. **(a)** Ultrasonographic (US) image of the liver shows an abscess as an oval anechoic area (arrowhead) with internal hyperechoic foci due to gas bubbles. **(b)** Coronal image from contrast-enhanced multidetector CT shows pneumobilia within dilated intrahepatic ducts (arrow) and gas within one of multiple liver abscesses (arrowheads). * = gallstone in the gallbladder. **(c)** Axial gadolinium-enhanced fat-saturated T1-weighted MR image shows an abscess (arrowhead), pneumobilia within dilated intrahepatic ducts (arrow), and thickened enhancing bile duct walls.

a.



b.

c.

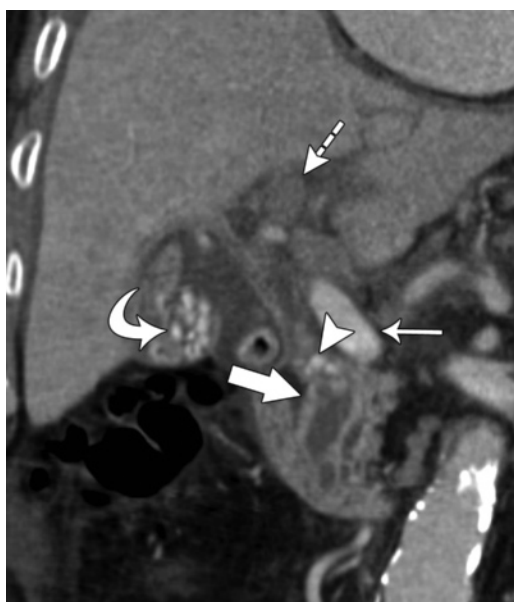


Figure 7. Portal vein thrombosis complicating BAC. Reformatted image from contrast-enhanced multidetector CT shows gallbladder stones (curved arrow) and choledocholithiasis (arrowhead). The main portal vein enhances proximally (thin straight solid arrow) but is occluded high in the porta hepatis due to thrombosis (dashed arrow). Note the thickened and enhancing CBD wall (thick arrow).

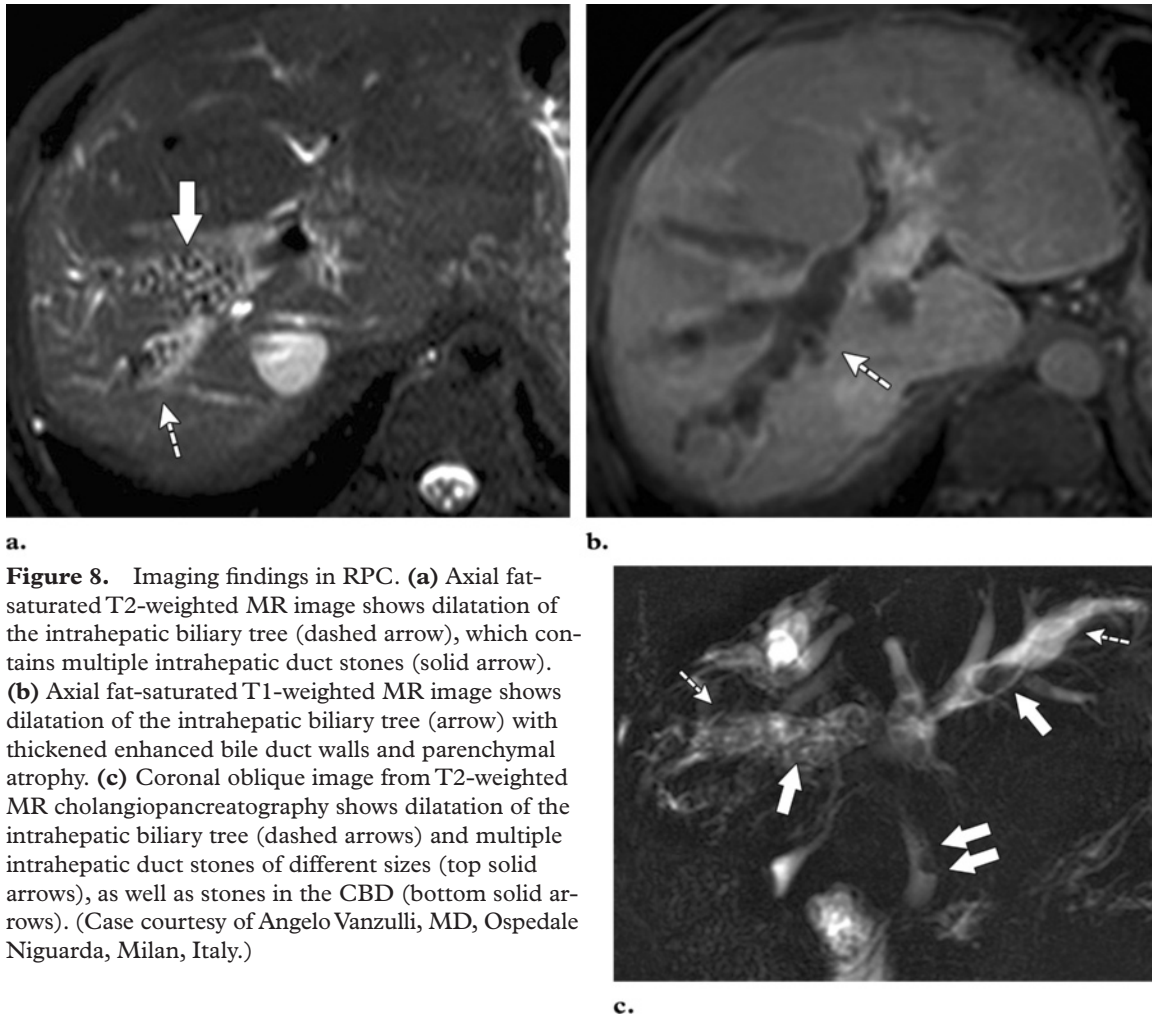


Figure 8. Imaging findings in RPC. **(a)** Axial fat-saturated T2-weighted MR image shows dilatation of the intrahepatic biliary tree (dashed arrow), which contains multiple intrahepatic duct stones (solid arrow). **(b)** Axial fat-saturated T1-weighted MR image shows dilatation of the intrahepatic biliary tree (arrow) with thickened enhanced bile duct walls and parenchymal atrophy. **(c)** Coronal oblique image from T2-weighted MR cholangiopancreatography shows dilatation of the intrahepatic biliary tree (dashed arrows) and multiple intrahepatic duct stones of different sizes (top solid arrows), as well as stones in the CBD (bottom solid arrows). (Case courtesy of Angelo Vanzulli, MD, Ospedale Niguarda, Milan, Italy.)

imaging, and contrast-enhanced dynamic and delayed high-resolution fat-saturated T1-weighted imaging.

Antibiotic therapy alone is inadequate for treatment and is associated with high mortality rates (87%–100%). Either endoscopic or percutaneous biliary drainage is necessary to decompress the biliary tree and thus minimize bacterial and endotoxin spillage into the bloodstream. Without biliary decompression, secretion of antibiotics into the biliary tree is limited, rendering their biliary concentration inadequate (7,17).

In the case of severe BAC, biliary decompression is performed emergently. In moderate to mild cases, conservative treatment is performed as the first option: broad-spectrum antibiotics and intravenous fluid are given. A response can

be expected in 70%–80% of the cases, allowing biliary decompression to be performed in a less urgent setting. Blood cultures should be performed before starting antibiotic administration. Although ampicillin and gentamicin are commonly used as the first-line wide-spectrum antibiotic regimen, they have been shown not to be ideal owing to widespread resistance. Currently, a combination of ureidopenicillin with metronidazole and an aminoglycoside or a combination of piperacillin plus tazobactam is the preferred treatment. Antibiotic therapy is usually continued for 7–10 days if the patient responds (2,7).

If the clinical picture does not markedly improve within 6–48 hours, endoscopic retrograde cholangiopancreatography (ERCP) or percutaneous transhepatic cholangiography (PTC) with biliary decompression is performed urgently (7,18).

Both ERCP and PTC are useful and safe decompression techniques, with a lower mortality rate than surgery (34% for surgery, 5%–10% for PTC, 10% for ERCP) and a higher success rate (82%–100% for PTC, 86%–100% for ERCP). Some authorities have recommended ERCP as the first-line therapy, pointing to the shorter hospitalization and less frequent occurrence of serious hemorrhage for patients treated with ERCP rather than with PTC (6,7,17,19).

PTC is the preferred modality for cases of high biliary obstruction, intrahepatic stones, previous biliary-enteric surgery, or failed endoscopic decompression (6,16). In practice, the choice between the two is based on the local expertise and the availability of resources (6,7,17,19).

Pregnancy and ascites constitute relative contraindications to PTC. Ascites can be treated with paracentesis prior to PTC. Coagulopathy, a relative contraindication to both ERCP and PTC, can be addressed with fresh frozen plasma and platelet transfusion. Pancreatitis, bowel perforation, and bleeding are the main complications of ERCP. External catheter discomfort and bleeding are the main disadvantages of PTC (9,11,20).

In patients unresponsive to drainage, the possibilities of inadequate drainage such as multifocal obstruction, cholecystitis, and hepatic abscess should be investigated with re-imaging (11,20).

Recurrent Pyogenic Cholangitis

Recurrent pyogenic cholangitis (RPC) is a progressive biliary disease characterized by recurrent episodes of bacterial cholangitis. It is associated with biliary tract ectasia, focal strictures, and formation of intrahepatic pigment stones (21).

Long-lasting intrahepatic duct obstruction or portal vein thrombosis may result in lobar or segmental atrophy. In the majority of patients, the left hepatic lobe is affected, although bilobar involvement is common (21).

Although most common in patients of Asian descent, a similar syndrome also occurs in other populations, including Latin Americans and Caucasians. Low socioeconomic status and rural environment seem to be associated with RPC (21,22).

Clonorchis sinensis and *Ascaris lumbricoides* infestations have been associated with RPC, but their etiopathogenic role has not been clearly demonstrated. One theory proposes that RPC arises from chronic infestations of the biliary tree. Persistent

inflammation and subsequent bile duct fibrosis lead to bile stasis, strictures, and pigment stone formation. These in turn result in progressive biliary obstruction and recurrent infections (23).

The prevalence of RPC is increasing in Western countries, partially due to increased awareness in the radiologic and surgical communities. Immigration from the Far East may also play a role (21).

The disease manifests as repeated episodes of bacterial cholangitis. Left untreated, RPC can result in liver abscesses, portal vein thrombosis, strictures, and intrahepatic stones. The bile ducts become chronically obstructed. Moreover, patients with RPC have an increased risk of cholangiocarcinoma (5%–18%) (21).

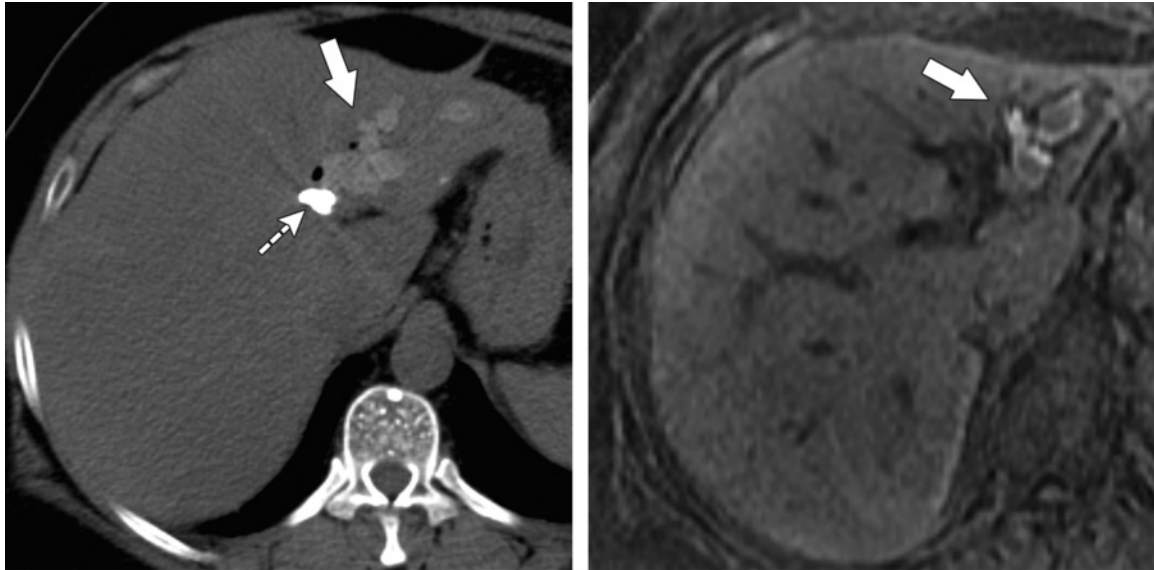
Diagnosis is based on a combination of clinical and imaging findings. **At imaging, RPC is characterized by stenosis or strictures of the peripheral ducts, with decreased branching and abrupt tapering (“arrowhead appearance”) associated with disproportionate dilatation of the central and extrahepatic bile ducts (Fig 8). Central dilatation tends to be diffuse, involving both stone-bearing and stone-free ducts. The periportal space is thickened owing to periductal inflammation and fibrosis (23,24).**

Stenotic areas are less than 1 cm in length and involve the intrahepatic ducts; stenoses rarely affect the extrahepatic biliary tree (23,24).

Intraductal stones are found in 80% of cases (Figs 8, 9). Owing to their proteinaceous composition, they may be hyperintense to the liver on T1-weighted images. On T2-weighted images, they appear hypointense to the liver. Small impacted calculi may manifest as duct irregularities (24).

Pneumobilia commonly occurs in RPC. It is due to stone passage across the ampulla with reflux of enteric gas into the biliary tree. It may also be due to gas-forming organisms within the biliary tree. It is easily diagnosed with CT, whereas at MR imaging it needs to be differentiated from stones. The nondependent position of the pneumobilia is useful for this purpose (23).

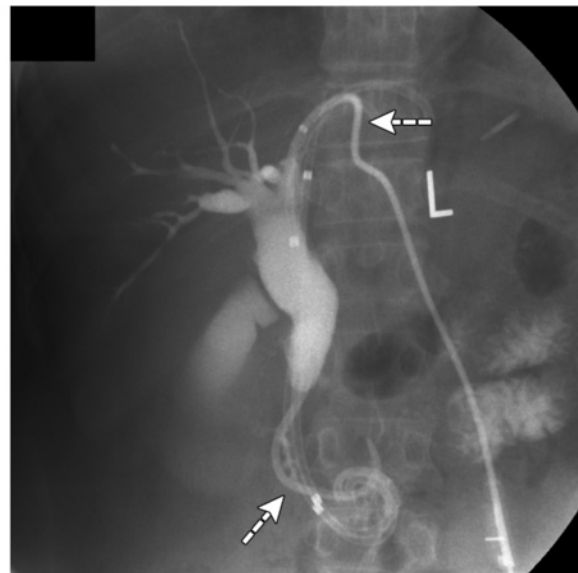
Parenchymal atrophy is a common manifestation of the chronic nature of the disease. Hepatic atrophy typically affects the left lobe or right posterior segments. The corresponding bile ducts are dilated and crowded. Parenchymal and bile duct wall enhancement, with blurred biliary duct contour, are observed in acute exacerbations (23–25).



a.

Figure 9. Imaging findings in RPC. (a) Axial image from nonenhanced multidetector CT shows pigment stones (solid arrow) in dilated left bile ducts; the stones appear partially calcified. Dashed arrow = biliary drainage catheters. (b) Axial nonenhanced fat-saturated T1-weighted MR image shows that the stones (arrow) are hyperintense relative to surrounding parenchyma. Note the associated atrophy of the left lobe. (c) Cholangiographic image, obtained by means of a transhepatic biliary drainage catheter (arrows) after percutaneous and endoscopic procedures for stone removal and stent placement, shows persistent ductal dilatation.

b.



c.

Abscesses are encountered in 20% of cases. They can be distinguished from bilomas owing to the presence of an enhancing rim (23–25).

Cholangiocarcinomas tend to occur in atrophied or heavily stone-burdened segments. Peripheral cholangiocarcinoma manifests as expansion of the affected segment. A low-attenuation mass with a thin rim of contrast enhancement and narrowing or obliteration of the portal vein should raise the suspicion of cholangiocarcinoma. Central cholangiocarcinoma manifests as a focal stricture with thickened enhanced walls (26). Follow-up with MR imaging is advised for early detection of cholangiocarcinoma.

Treatment is directed to control the acute episodes of cholangitis and to remove the pre-

disposing causes. Treatment of biliary stones and strictures often requires a multidisciplinary team of radiologists, endoscopists, and surgeons (21).

Treatment of acute episodes is similar to that described for non-RPC cases of acute bacterial cholangitis and includes endoscopic or radiologic biliary drainage, antibiotics, and supportive measures (21).

Accurate delineation of biliary anatomy with ERCP, MR imaging, or CT is mandatory for treatment planning. ERCP, PTC, and surgery are not mutually exclusive.

Localized disease or first presentations are treated with endoscopic or percutaneous drainage, biliary stone removal, or stricture dilatation (Fig 9). Surgery is reserved for cases in which both ERCP and PTC have been unsuccessful. ERCP has been proved very successful in stone clearance in patients with RPC and stones principally located in the CBD. Alternatively, a combination of PTC biliary drainage followed by surgical stone extraction allowed complete stone clearance in 94% of patients at 60-month follow-up in one series (21,27).

In the case of diffuse intrahepatic disease or in the case of residual disease after ERCP or PTC, surgery is the preferred treatment. Surgical therapy is based on biliary exploration with stone extraction, choledochojejunostomy, or lobar or segmental liver resection. At completion, a common surgical procedure is the construction of a Hutson loop, a Roux-en-Y choledochojejunostomy fixed to the anterior abdominal wall with radiopaque markers, to facilitate imaging-guided extraction of residual or recurrent intrahepatic stones. Stone clearance can be achieved in 96% of the cases (21).

PTC and ERCP are options for recurrent disease after surgery. Moreover, interventional radiology is the mainstay of treatment of liver abscesses occurring in treated and untreated RPC (21).

Intrahepatic pigment stones, strictures, duct dilatation, segmental atrophy, and pneumobilia are found both in acute episodes and in silent disease. However, ductal and parenchymal enhancement are observed in acute episodes.

Parasites

Clinical manifestations vary with specific parasites. In cases of bacterial superinfection, the clinical picture can be indistinguishable from BAC. Nonetheless, imaging, stool examination, presence of eosinophilia, and serology may help identify an underlying parasitic infection.

Echinococcosis.—*Echinococcus granulosus* and *Echinococcus multilocularis* are cestodes that respectively infest dogs and foxes as definitive hosts and sheep and rodents as intermediate hosts. *E granulosus* is found mainly in the Mediterranean area, Russia, Australia, and South America. *E multilocularis* is endemic in the northern hemisphere, infesting forested regions in northern parts of Europe, Asia, and America. These para-

sites can accidentally infect humans as intermediate hosts, owing to ingestion of vegetables or water contaminated by their eggs. In the human intestine, embryos are released from ingested eggs, penetrate the bowel mucosa, and are carried through the portal venous system to the liver. There, they give rise to parasitic cysts. Less commonly, the embryos can disseminate to the lung or other organs (28,29).

In intermediate hosts, *E granulosus* gives rise to a unilocular expanding hydatid cyst, composed of an inner germinal layer and outer acellular laminated layer. The cyst is encapsulated by a fibrous capsule produced by the host and called the pericyst. The brood capsule and protoscolices bud inward from the peripheral germinal layer. The internal growth of daughter cysts is responsible for the characteristic spoke-wheel pattern at imaging. With the parasite's death, the endocyst detaches (water lily sign) and the cyst calcifies. Untreated echinococcal cysts expand by compression of surrounding liver tissues, leading to symptoms by mass effect. Without intervention, their pressure can exceed that of the biliary tree, causing rupture or fistulizing into the biliary ducts (5%–30% of cases) with resultant cholangitis and spontaneous cyst decompression. Less commonly, rupture into the peritoneum can result in peritonitis and even anaphylaxis. The fatality rate is 2.2% (28–31).

Diagnostic imaging plays a pivotal role in diagnosis of cystic echinococcosis. Because of antigenic cross-reactivity with other parasites, serology has an ancillary role and requires the use of a combination of tests to increase its sensitivity and specificity (29).

Imaging findings of echinococcosis caused by *E granulosus* reflect the different stages of the hydatid cyst. During its early stages, the hydatid cyst appears as a simple cyst at CT, although a laminated wall (double line sign) or free-floating scolices (snowflakes sign) may be demonstrated at US. At MR imaging, a fibrous persistently hypointense rim is seen. With the development of daughter cysts, a spoke-wheel appearance is observed. At CT, the attenuation of daughter cysts is lower than that of the mother cyst because the latter contains free-floating scolices. At MR imaging, the daughter cysts are less hypointense on T1-weighted images than the mother cyst. If

Teaching
Point

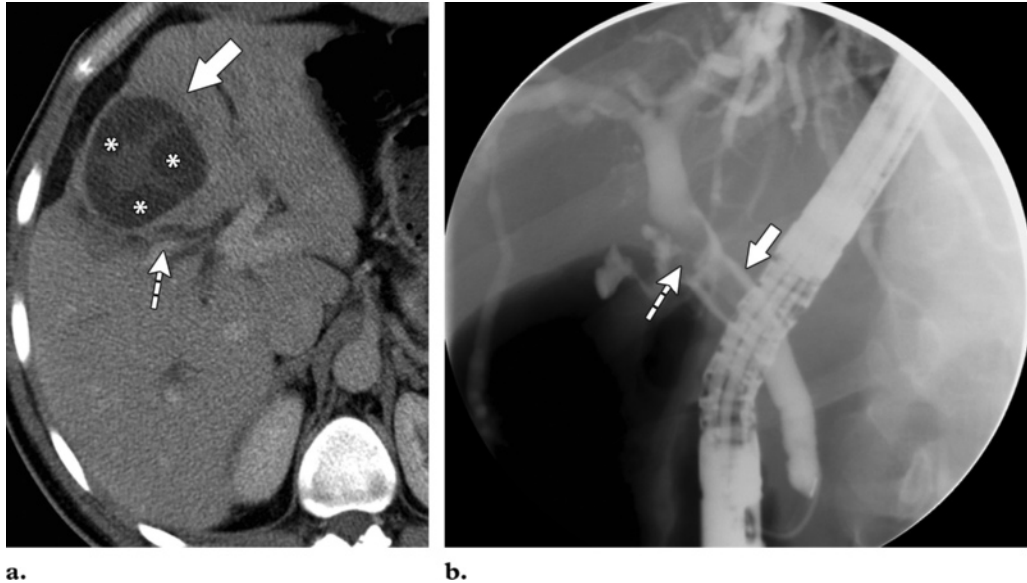


Figure 10. Hydatid disease due to *E granulosus*. **(a)** Axial contrast-enhanced CT image shows the typical spoke-wheel appearance of *E granulosus* (solid arrow), with multiple daughter cysts (*) surrounding a central matrix. Note the intrahepatic biliary dilatation (dashed arrow). **(b)** Image from ERCP shows intra- and extrahepatic biliary duct dilatation and a balloon catheter (dashed arrow), which is being used to retrieve an intraductal daughter cyst (solid arrow). Echinococcal membranes were recovered during the procedure.

the parasite dies, intracystic pressure is reduced, and the membranes detach and fall into the cyst, where they appear as wavy lines (water lily sign). The dead cyst then undergoes progressive shrinkage and calcification (28).

In biliary echinococcosis, imaging findings are characterized by biliary duct dilatation that can extend to the peripheral biliary ducts, cystobiliary fistulas, and filling defects in the biliary tree (Fig 10). Filling defects are due to daughter cysts or hydatid membranes, with the latter having a characteristic leaflike irregular appearance (30,31).

Treatment is often staged. Patients receive albendazole, with disappearance of cysts in 48% of cases and reduction in size in 24%. Persistent or nonresponding cysts can be managed with image-guided drainage provided the cyst is unilocular and there is no communication with the biliary tree. Unilocular cysts that do not respond to systemic therapy have been treated with percutaneous drainage followed by instillation of absolute ethanol or hypertonic saline as a scolical agent. Percutaneous treatment is as effective as surgical pericystectomy. Cyst aspira-

tion is contraindicated when cysts are superficial, calcified, solid, multilocular, or communicate with the biliary tree. Surgery is considered in the case of large cysts or when there is impending superinfection, rupture, critical location, or failure of other treatments. In the case of jaundice or cholangitis, biliary drainage performed either radiologically or with ERCP is mandatory. Intra-biliary daughter cysts and hydatid membranes can be extracted during ERCP (29,32,33).

E multilocularis infection is characterized by multilocular alveolar cysts, with exogenous proliferation and surrounding tissue invasion. Unlike *E granulosus* infection, there is no host pericyst. Instead, alveolar hydatid disease manifests as ill-defined infiltration that elicits an intense fibrotic reaction. The inflammatory process directly involves the biliary tree and portal vein branches, leading to subsequent biliary dilatation and parenchymal atrophy. Involvement of hepatic veins can cause secondary Budd-Chiari syndrome. The disease is often clinically silent for many years. Ultimately, it manifests clinically as epigastric pain, jaundice, or weight loss and fatigue. The fatality rate for untreated or inadequately managed cases is high (28,29).

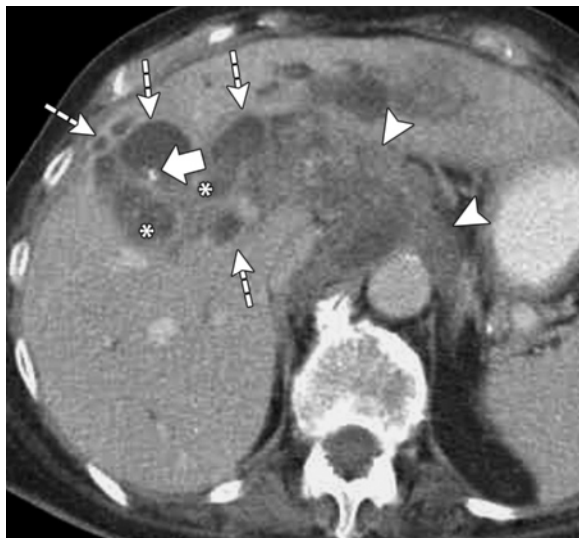


Figure 11. Alveolar hydatid disease (*E multilocularis* infection). Axial contrast-enhanced CT image shows multiple hypoattenuating lesions within the hepatic parenchyma (*), which represent necrotic tissue, and some cysts (dashed arrows), which represent vital metacestodal vesicles. Note the associated calcifications (solid arrow). Parasitic tissue (arrowheads) infiltrates the retroperitoneum and hepatic hilum, partially encasing the aorta.

At imaging, *E multilocularis* appears as an ill-defined infiltration with nonenhancing solid and cystic areas (Figs 11, 12). The cystic areas mainly represent liquefactive necrosis or parasitic vesicles, while the solid components represent areas of coagulative necrosis or granulomas and can undergo calcification. T2-weighted sequences are helpful to demonstrate the small parasitic cysts usually found in or adjoining the more obvious solid component. Biliary dilatation due to hilar infiltration or direct parasitic biliary invasion can be depicted at MR imaging (28,34).

Treatment is surgical, with partial hepatectomy if possible or liver transplantation. Long-term albendazole adjuvant chemotherapy increases the 10-year survival up to 80%, whereas surgery alone is associated with a 10-year survival of less than 25% (29).

Clonorchiasis and Opisthorchiasis.—*C sinensis*, *Opisthorchis viverrini*, and *Opisthorchis felinus* are closely related trematodes with similar life cycles and similar biliary pathophysiology. *O felinus* predominates in Siberia, *O viverrini*



Figure 12. Alveolar hydatid disease (*E multilocularis* infection). Coronal oblique image from T2-weighted MR cholangiopancreatography shows multiple small filling defects (arrow) within the dilated bile ducts. The filling defects represent metacestodal vesicles.

in Thailand and Laos, and *C sinensis* in the Far East (35).

The metacercariae, ingested with undercooked freshwater fish, encyst in the stomach and enter the biliary tree through the ampulla of Vater. They migrate in the small and medium-sized biliary ducts, where they become established and proliferate for decades (35,36).

Patients are usually asymptomatic until parasite burden becomes high (>100 in the case of clonorchiasis). Owing to their small size, the parasites seldom cause obstruction of large ducts. Instead, they cause chronic inflammation with subsequent adenomatous hyperplasia and periductal fibrosis. Heavy infestations by parasites can cause obstruction of small peripheral ducts with resultant cholangitis (35,36).

Involvement of the peripheral ducts with sparing of the extrahepatic ducts is characteristic of these infestations. Peripheral small bile ducts show evidence of chronic inflammation, dilatation, and wall thickening. In some patients, there is diffuse uniform dilatation of the entire peripheral biliary tree. Extrahepatic biliary ducts and

the gallbladder are affected by heavy parasite burdens. Floating flukes, up to 1 cm in size, can be visualized with imaging (Fig 13). Even in these cases, duct caliber is normal or just minimally increased (35–37).

Bacterial cholangitis, biliary stones, cholangiocarcinoma (Fig 14), and RPC may complicate clonorchiasis and opisthorchiasis (35,36).

Treatment is mainly based on biliary decompression with ERCP or PTC in the case of acute cholangitic episodes, together with administration of praziquantel or bithionol (36).

Fascioliasis.—*Fasciola hepatica* is a trematode liver fluke whose miracidia, after having infested freshwater snails, multiply and emerge as cercariae. Excreted metacercariae are ingested by sheep or cattle, their normal host; humans are infested only accidentally by ingesting contaminated water or vegetables. Metacercariae encyst in the stomach, perforate the duodenal wall, and migrate into the peritoneal cavity. Subsequently, they perforate the liver capsule and penetrate into the liver. During this “hepatic phase,” the fluke digests hepatocytes, leading to clusters of peripheral, small, sterile necrotic cavities and abscesses. They have a typical serpentine arrangement that persists for many months or even years.

After a few months in the liver, the parasites become established in the biliary ducts. During this “biliary phase,” the flukes mature and start releasing eggs into the biliary tree. They can live in the biliary tree for decades. At first they reside in smaller biliary branches, but as they grow, they move toward the central and extrahepatic biliary tree and the gallbladder. They cause biliary inflammation, bile duct wall thickening, and intra- and extrahepatic biliary dilatation (35,38,39).

In the hepatic phase, fever, abdominal pain, and hepatomegaly dominate the clinical picture; eosinophilia is almost always found. In the biliary phase, biliary colic or cholangitis is encountered (39).

The disease is common in the underdeveloped world, but can also be encountered in Europe and the United States. In nonendemic areas, fascioliasis can be overlooked. Eosinophilia will nearly always be present to suggest the possibility



Figure 13. Biliary flukes (*C. sinensis*). T-tube cholangiogram shows biliary worms as small, comma-shaped filling defects (arrows).

of a parasitic infestation, which would then need to be confirmed with serologic tests and CT or MR imaging of the abdomen (39).

CT is the most used imaging technique for diagnosis of fascioliasis. In the hepatic phase, multiple serpentine, branching, hypoattenuating subcapsular lesions pointing toward the central liver as well as multiple clustered hypoattenuating nodules (tunnels and caves sign) are typical imaging features (Fig 15). In many cases the entire path of migration, from the entry site at the hepatic capsule to the central liver, will be visible (35,39).

In the case of biliary fascioliasis, US or ERCP can show intrabiliary filling defects and biliary dilatation. Parasites move spontaneously and do not shadow at US. Extrahepatic ducts and the gallbladder wall are thickened. Coexistent hepatic phase liver abnormalities can be helpful to clarify the biliary findings (35,39). Bithionol or triclabendazole is the treatment of choice (39).

Ascariasis.—The giant roundworm *A. lumbricoides* affects 25% of the world population. It is common in tropical and subtropical areas, but ascariasis is the third most common helminthic infection in the United States after hookworm and trichuriasis (40).

Ingested eggs release their larvae in the duodenum. These then traverse the duodenal wall and

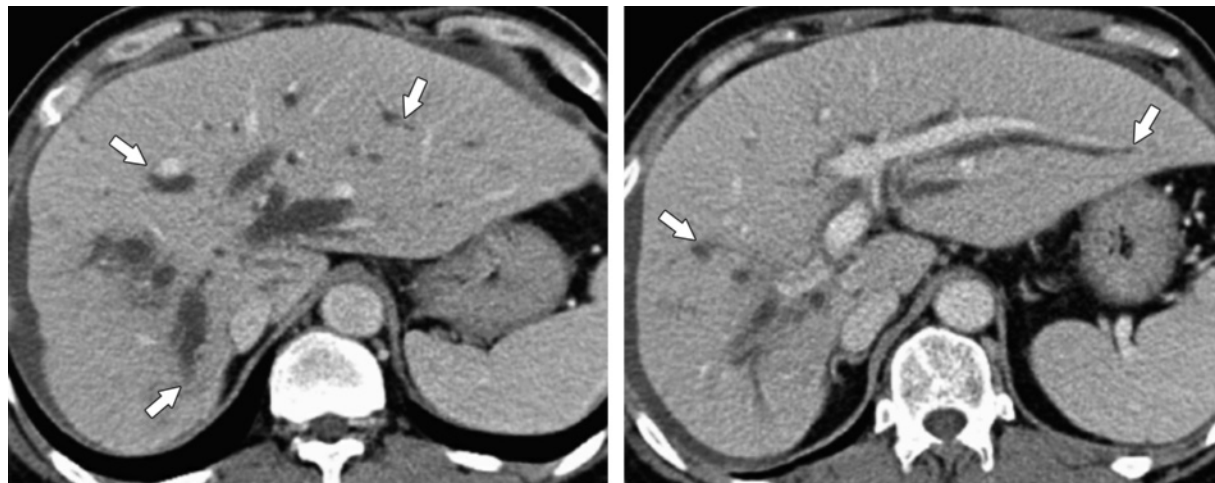


Figure 14. Opisthorchiasis complicated by cholangiocarcinoma. CT images (**a** obtained at a higher level than **b**) show irregular dilatation of the intrahepatic bile ducts (arrows). Ova of *O viverrini* were found in the stool. The patient was considered to have cholangiocarcinoma on the basis of elevated levels of serum tumor markers and was treated with biliary bypass. The patient refused hepatectomy. (Case courtesy of Julaluck Promsorn, MD, Khon Kaen, Thailand.)



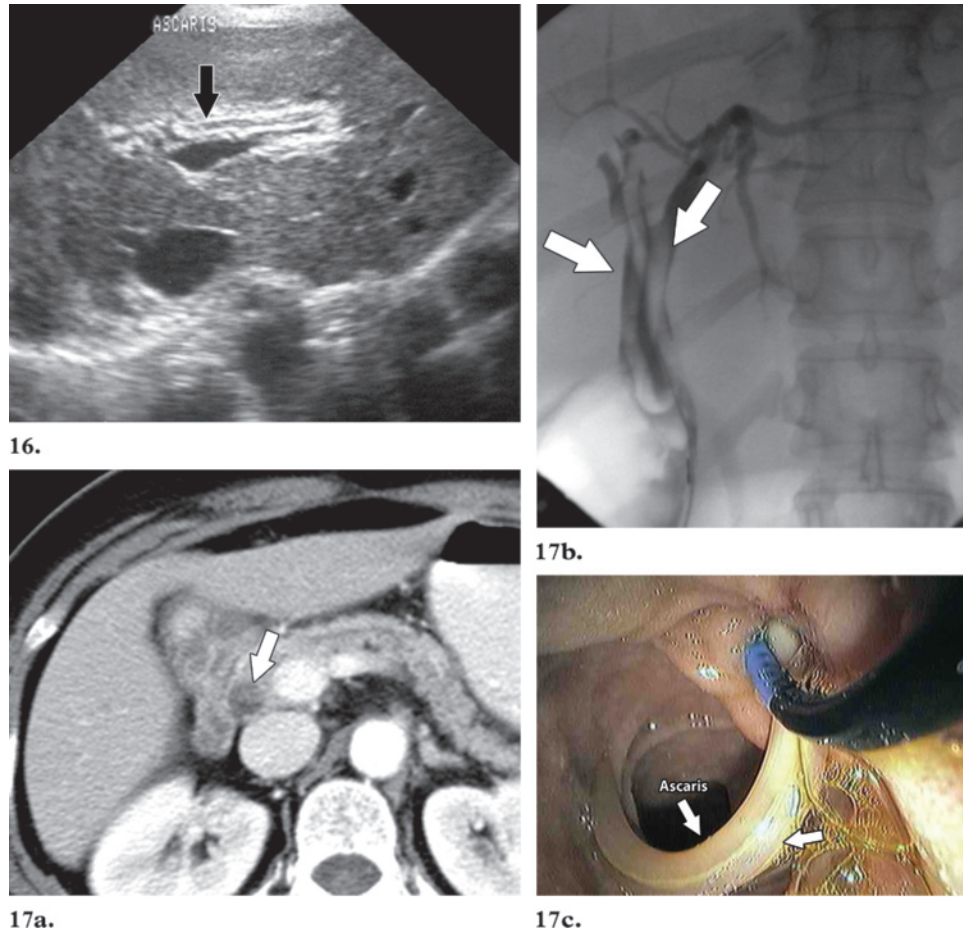
Figure 15. Liver flukes (*F hepatica*). Axial contrast-enhanced CT image shows the tunnels and caves sign (arrows), a finding typical of *F hepatica*. This sign consists of serpentine tubular and nodular hypoattenuating areas from the peripheral to the central liver. It represents sterile necrosis of hepatic tissue digested by the parasite.

gain access to the bloodstream. From the pulmonary vasculature they penetrate the alveoli. Eventually they enter the bronchi and trachea and are ultimately swallowed. The larvae mature in the small bowel, where the adults produce their eggs,

passed in the feces. *A lumbricoides* are very mobile organisms that tend to explore and penetrate all the possible orifices. They gain access to the biliary and pancreatic ducts (40–43). In adults, they can settle in the CBD. This is especially true in patients who have undergone cholecystectomy and those who have undergone biliary exploration or biliary surgery (40,42,43). The biliary ectasia that results from previous biliary surgery may account for this predilection.

Secretions from *Ascaris* induce sphincter of Oddi spasm with resultant biliary colic. The subsequent biliary stasis, along with intestinal bacteria brought by the parasite, can trigger pyogenic cholangitis or cholecystitis. When worms gain access to the intrahepatic biliary tree, necrosis and abscesses can ensue. Moreover, parasite secretions that are rich in β -glucuronidase, eggs, and dead parasites promote stone formation. RPC can occur in up to 5% of patients with biliary ascariasis (40,43).

Ascariasis is diagnosed on the basis of fecal examination. Diagnostic imaging, mainly US, is of paramount importance in the diagnosis of biliary involvement in ascariasis (41,42).



Figures 16, 17. Ascariasis due to *A lumbricoides*. **(16)** US image shows the *Ascaris* worm as an elongated hypoechoic structure with hyperechoic walls (arrow) within the intrahepatic biliary tree. **(17a)** Axial contrast-enhanced CT image shows the *Ascaris* worm (arrow) as a nondependent, mildly hyperattenuating filling defect in the distal CBD. **(17b)** ERCP image shows the nature of the filling defect seen at CT. The worm appears as a long filling defect folded on itself (arrows) in the opacified duct. **(17c)** Endoscopic photograph of the duodenum shows the worm (arrows) during endoscopic extraction.

Ascaris worms appear as elongated intrabiliary filling defects, coiled up or parallel to the biliary duct, which may slowly move at real-time imaging (Figs 16, 17). At US, they have echogenic walls and a hypoechoic center, devoid of shadowing. At CT, they are hyperattenuating relative to bile; at MR imaging, they exhibit low signal intensity on T2-weighted images. Occasionally, the fluid-filled gastrointestinal tract of worms may appear hyperintense on T2-weighted images. The gallbladder may be distended and the biliary ducts dilated, with edematous walls (40,41,44).

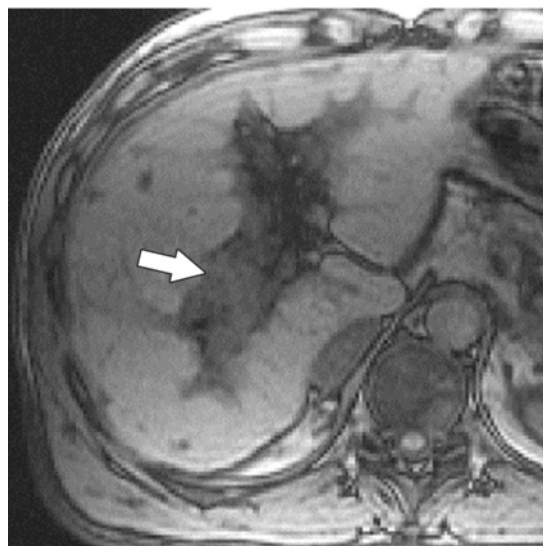
When acute cholangitis complicates the ascariasis, treatment with biliary drainage and antibiotics takes priority over addressing the underlying parasites. After the acute cholangitis has subsided, the *Ascaris* can be eradicated with medications, ERCP, or even surgery. Praziquantel is an effective antiparasitic therapy, whose efficacy is

evaluated by means of serial US examinations. When medications fail to eradicate the infection, ERCP is used to directly visualize and remove the worms. This helps prevent cholangitis and stone formation. Surgery is reserved for endoscopic failures and intrahepatic duct ascariasis (40,43).

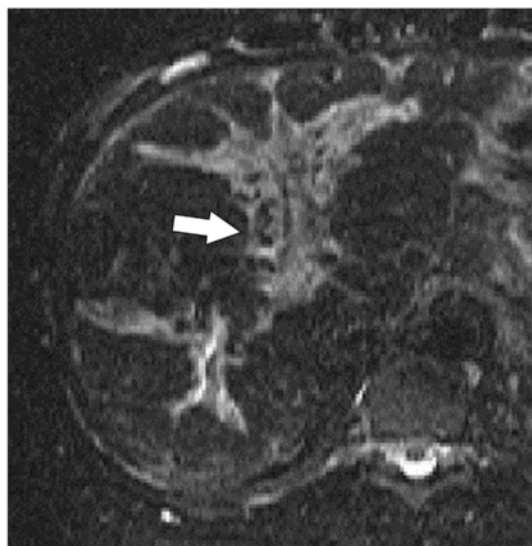
Schistosomiasis.—*Schistosoma mansoni* and *Schistosoma japonicum* are trematodes that parasitize abdominal veins and exhibit similar pathophysiology. *S mansoni* is found in South America, Africa, and the Middle East, whereas *S japonicum* is common in the Far East. *Schistosoma* infects humans after direct contact with contaminated fresh water. In fact, their cercariae are able to penetrate intact human skin. From skin entry, the parasites migrate to the lungs and subsequently gain access to the portal venous system, where they mature and mate. The mated worms subsequently migrate to the venular tributaries.



a.



b.



c.

Figure 18. Schistosomiasis. (a) US image of the liver shows hyperechoic periportal thick fibrous bands (arrow), a typical finding of schistosomiasis. (b) T1-weighted MR image shows the hypointense fibrous bands (arrow) extending from the hepatic hilum toward the periphery. (c) Axial fat-saturated T2-weighted MR image shows that the fibrous bands (arrow), which are due to persistent low-grade inflammation, are hyperintense relative to liver parenchyma. (Case courtesy of Robert Kane, MD, Beth Israel Deaconess Medical Center, Boston, Mass.)

In the case of *S mansoni*, migration is via tributaries of the superior mesenteric vein. *S japonicum* invades tributaries of the inferior mesenteric and superior hemorrhoidal veins. In these sites, the parasites release eggs that seed the liver via the portal vein. Eggs become trapped in the periportal venous space and along the Glisson capsule, where they elicit a chronic granulomatous inflammation with abundant fibrosis. Some eggs undergo calcification. Chronic inflammation leads to widespread periportal fibrous thickening with resultant cirrhosis (clay pipe stem fibrosis) and portal hypertension (45,46).

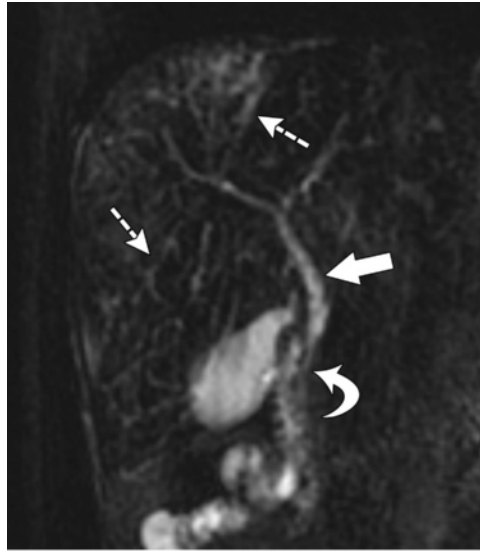
Biliary involvement is secondary to intense periportal fibrosis with subsequent biliary obstruction, a paucity of second- and third-order biliary branches, and bile duct proliferation (47,48).

In the case of *S mansoni*, the eggs are large and rarely calcify; their deposition and the subsequent periportal fibrosis are most prominent in the central liver. The liver is traversed by thick fibrous bands radiating from the hilum, and its

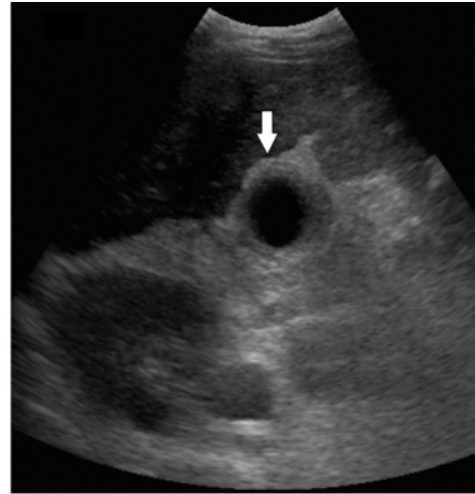
surface resembles a “turtle back.” The eggs of *S japonicum* are small and tend to disseminate to the periportal space of peripherally located portal venules near the liver capsule. Moreover, they tend to calcify. When this occurs, the periportal fibrosis is more widespread and the fibrous bands are less prominent than those of *S mansoni*. The fibrous strands have a uniform polygonal “honeycomb” fibrotic appearance. Calcifications are commonly seen (46).

Initial symptoms are nonspecific, comprising fever, headache, myalgia, bloody diarrhea, and abdominal pain. Eosinophilia is a common finding. Late manifestations are related to liver cirrhosis and biliary obstruction (45,47).

In *S mansoni* infestation, imaging is dominated by thick fibrous bands around portal vein branches (Fig 18). The liver is usually shrunken with a nodular surface, which correlates with the turtle back appearance at pathologic examination (46).



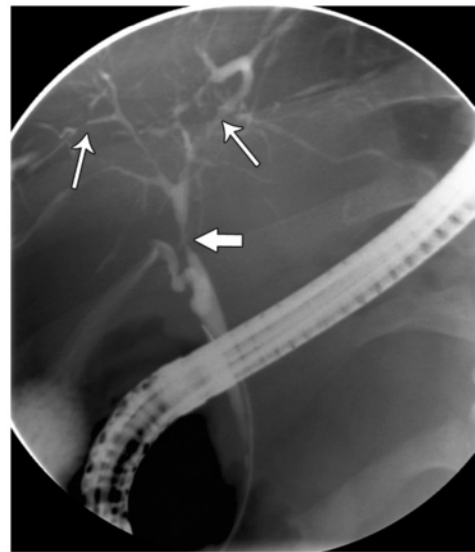
19.



20b.



20a.



20c.

Figures 19, 20. HIV-related cholangitis. (19) Coronal oblique image from T2-weighted MR cholangiopancreatography shows pruning and dilatation of intrahepatic ducts (dashed arrows), edematous folds in the CBD (straight solid arrow), and sphincter of Oddi stenosis (curved arrow). (20a) US image of the liver shows thickened bile duct walls (arrow). (20b) Transverse US image shows thickening of the gallbladder wall (arrow). (20c) ERCP image shows strictures and dilatation of intrahepatic ducts (thin arrows) and a long extrahepatic duct stricture (thick arrow). Long extrahepatic duct strictures and sphincter of Oddi stenosis are considered distinguishing features of HIV-related cholangitis.

In *S japonicum* infection, typical imaging findings include a polygonal pattern of periportal fibrosis that resembles fish scales and calcification of interlobular septa (46).

Owing to the chronic granulomatous inflammatory nature of the fibrotic changes in both *S mansoni* and *S japonicum* infection, they tend to appear hyperintense on T2-weighted images and to enhance after contrast material administration (46,49).

Biliary findings tend to manifest at MR cholangiopancreatography before the detection of laboratory findings of cholestasis. The imaging findings include areas of focal narrowing, a paucity of second- and third-order biliary branches, and irregularities in the contours of biliary ducts (48).

Diagnosis is based on detection of eggs in multiple fecal examinations and on the imaging findings. It has been demonstrated that US is useful for both detection and quantification of the hepatosplenic disease. Serology is less sensitive and less specific (45). Praziquantel is used to treat the infestation (45).

Cholangitis in Immunocompromised Patients

HIV-related Cholangitis

The liver and biliary tree are targets of infections in human immunodeficiency virus (HIV)-positive patients. The biliary tree tends to be affected in patients with markedly depressed immune function, with a CD4 count less than 100/mm³. The clinical findings are nonspecific but often include right upper quadrant pain and abnormal results on liver function tests. The latter are commonly observed in HIV patients and can be multifactorial, ranging from drug reactions to hepatitis. Fever and chills could be signs of BAC or any systemic infection, whereas jaundice is rarely encountered unless there is marked liver dysfunction or high-grade CBD obstruction. Therefore, imaging plays a crucial role in assessing HIV patients suspected to have liver or biliary infections (50,51).

Acquired immunodeficiency syndrome (AIDS) cholangiopathy is a form of secondary sclerosing cholangitis that affects patients who are severely immunocompromised. It may result from opportunistic biliary infections affecting the biliary ducts or causing ischemia or autonomic nerve damage, but can also arise from direct invasion of biliary epithelium by the HIV itself (50,51).

In 50% of cases, no definite pathogen is identified; in the remaining cases, a plethora of agents have been implicated, including cytomegalovirus, *Cryptosporidium parvum*, *Mycobacterium avium* complex, and herpes simplex virus. Symptoms are usually nonspecific and represented by right upper abdominal pain and elevated transaminase levels. The alkaline phosphatase level can be as high as 20 times the normal range, while the bilirubin level is normal or only mildly elevated. The pain can be so severe as to require narcotics. Many different diseases enter the differential diagnosis, mainly parenchymal liver processes like hepatic *M avium* complex infection. Imaging and biopsy are required for definite diagnosis (50–52).

Imaging findings resemble those of sclerosing cholangitis but are associated with papillary stenosis and long extrahepatic bile duct strictures. Typical features include intra- and extrahepatic biliary dilatation with predominant left-sided biliary involvement. Other findings include saccular dilatations, debris, pruning, irregular thickening of the CBD, papillary stenosis, and acalculous cholecystitis (Figs 19, 20). The bile duct and gallbladder walls are usually thickened. Diagnosis is based on duodenal or papillary biopsy, with the results showing biliary inflammatory changes and the associated pathogens (51–56).

Treatment is based on sphincterotomy, biliary stent placement, and stricture dilatation. Bactrim (sulfamethoxazole and trimethoprim) and ganciclovir are useful to treat *C parvum* and cytomegalovirus infections, respectively (50).

Cholangitis in Liver Transplant Recipients

Cholestasis is a common problem after orthotopic liver transplantation (OLT). Causes include acute or chronic rejection, ischemia, drugs, preservation injury, biliary obstruction, and infection. Viral, fungal, or bacterial infections in the liver, in other organs, or systemic all belong to the differential diagnosis (57,58).

A tight biliary anastomosis may be a predisposing factor for the occurrence of anastomotic strictures (59).

Parenchymal liver biopsy can be helpful to clarify the cause of cholestasis in OLT. Histologic sampling helps assess for ischemia, drug reactions, or rejection. On the other hand, obstructive cholangitis cannot be documented unequivocally with biopsy. The same histologic pattern can be seen in biliary obstruction, biliary leaks, ischemia, and systemic bacterial and viral infections. Moreover, severe systemic infections are associated with marked obstructive cholangitic response of the liver, which is pathologically indistinguishable from that induced by biliary obstruction (57). Therefore, imaging is usually required for diagnosis of obstructive cholestasis and of cholangitis in OLT patients (57).

Cholangitis lenta (subacute nonsuppurative cholangitis) represents a nonacute response of the liver to systemic bacterial or fungal infections. It is an important cause of liver failure and mortality in OLT patients. There are no specific imaging or clinical findings. Blood and biliary cultures are noncontributory. Pathologic findings include proliferation of bile ductules at the portal tract edges, absence of acute inflammatory changes, and a normal nonreactive structure of the interlobular bile ducts. Imaging is performed to exclude obstruction and other causes of cholestasis. Liver biopsy is mandatory for diagnosis (58).

Positive bacterial culture of bile in OLT is particularly common (73%). In contrast to non-transplant recipients, bacterial cultures in OLT grow out gram-positive bacteria, mainly enterococci. Moreover, cholangitis has been reported in 18% of OLT patients and plays an important role in the occurrence of bacteremia (19% of patients) and of liver abscesses (4% of patients). Bacterial

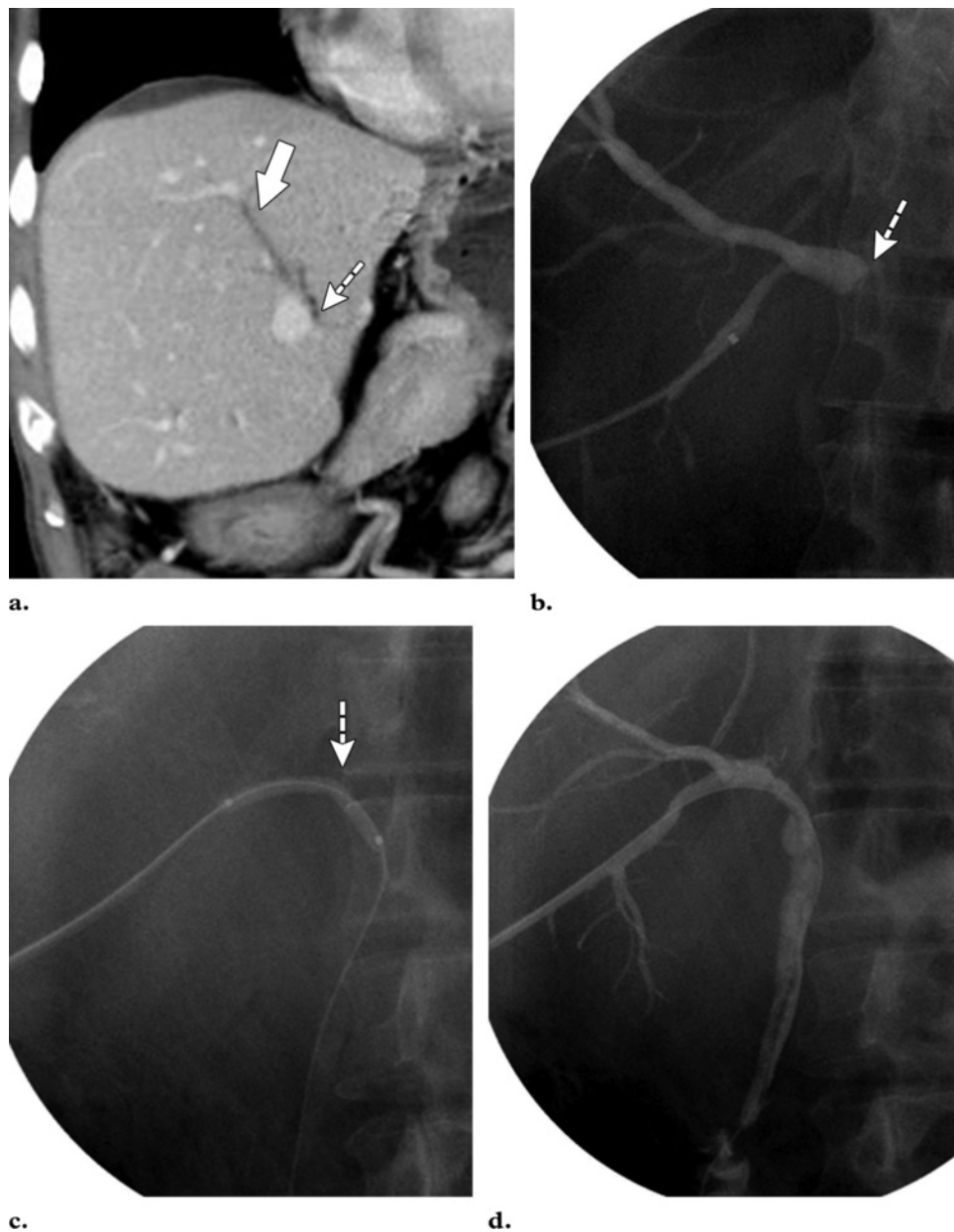


Figure 21. BAC after OLT. **(a)** Coronal contrast-enhanced multidetector CT image shows focal intrahepatic bile duct dilatation (solid arrow) and stenosis (dashed arrow). **(b)** Transhepatic cholangiogram obtained by means of a percutaneous biliary drainage catheter shows the focal intrahepatic bile duct dilatation and stenosis (arrow). **(c)** Cholangiogram shows percutaneous balloon dilation (arrow) being performed at the site of the focal stricture to reestablish biliary drainage. **(d)** Postprocedure cholangiogram shows resolution of the stricture, with free flow of contrast material into the duodenum.

cholangitis after OLT has a bimodal distribution, with the first peak occurring after 4 weeks and the second one after 17 weeks. *Candida*-associated cholangitis occurs much less often than its bacte-

rial counterpart (<1% of OLT patients), and its frequency peaks early in the posttransplantation period (60–62).

Numerous factors predispose OLT patients to bacterial colonization of the biliary tree, which

can lead to cholangitis and sepsis. These factors include the immunosuppressed state of the patients, altered biliary motility with decreased biliary clearance of ascending bacteria, use of plastic biliary stents, and anastomotic or nonanastomotic strictures. Less common factors are stone formation, use of T tubes, and papillotomy (60,61,63,64).

In OLT patients, owing to the common occurrence of bacterial colonization and the nonspecific elevations of liver function test results, alkaline phosphatase, and white blood cell count, the diagnosis of cholangitis is more challenging (60).

Documentation of biliary obstruction helps support the diagnosis. Although it constitutes a prerequisite for development of cholangitis, the associated biliary dilatation is often less pronounced and more difficult to ascertain with imaging in OLT cases. For this purpose, the performance of US is low (sensitivity, 38%); MR cholangiopancreatography (sensitivity, 80%–100%), PTC, and T-tube cholangiography are all more sensitive (63,65–69).

Imaging allows biliary mapping, assessment of vascular patency, and planning of subsequent treatments. Besides multiantibiotic regimens, chosen on the basis of local experience and the sensitivity of the cultured bacteria, biliary drainage and stricture dilatation may be lifesaving (Fig 21). PTC or ERCP drainage is chosen according to the specific type of biliary anastomosis and to the location and number of strictures. When minimally invasive treatments fail, re-transplantation may be the only option (60–63,66,70).

Cytomegalovirus causes one of the most common viral infections of the biliary tree in OLT patients. Cytomegalovirus usually establishes a latent infection in many cells, including biliary epithelial cells and endothelial cells of the adjacent vessels. This causes inflammation of the intra- and extrahepatic biliary tree with features indistinguishable from those of HIV-related cholangitis. A strong association between cytomegalovirus infection and biliary complications in OLT patients has been demonstrated, including extrahepatic strictures requiring biliary reconstruction. Indeed, 31% of patients infected with cytomegalovirus develop strictures. The diagnosis is based on documentation of cytomegalovirus pp65 antigenemia and immunohistochemistry. Treatment is aimed at relieving the obstruction, usually by

means of stent placement, and overcoming the infection with ganciclovir. If this approach fails, biliary reconstruction or even re-transplantation must be considered (71–73).

Other rarer types of cholangitis have been described in OLT patients and in patients undergoing aggressive immunosuppression. These include adenovirus ascending cholangitis and *C parvum*-associated sclerosing cholangitis (74,75).

Adenovirus is a known cause of necrotizing hepatitis in OLT and in severely immunosuppressed patients. It has occasionally been reported as responsible for necrotizing cholangitis involving the interlobular bile ducts, with or without associated necrosis of surrounding hepatocytes. In the few reported cases, no imaging features were described; the diagnosis was established with liver biopsy, viral cultures from stool, and bowel wall biopsy (74).

Although *C parvum*-associated sclerosing cholangitis is common in HIV patients, it has rarely been reported in OLT patients undergoing immunosuppression with tacrolimus and prednisone. It is likely related to CD4 depression. Histologic results are characterized by hepatic fibrosis, bile duct proliferation, and inflammatory infiltrate. Stools are positive for *C parvum*. In the very few reported cases, imaging revealed dilatation and irregularity of the intrahepatic bile ducts in association with variable patterns of obstruction caused by anastomotic strictures, multiple intrahepatic strictures, or CBD kinking. However, in early stages the biliary system may appear normal at imaging. *C parvum* may be histologically visible lining the ductal epithelium. Treatment is based on biliary revision, paromomycin, and azithromycin (38,75,76).

Conclusions

Diagnostic imaging plays an important role in biliary infections, helping establish the diagnosis and reveal possible complications. Interventional radiology is useful in treatment of affected patients.

A summary of the most important features of infectious cholangitis is provided in the Table.

Most Important Features of Different Types of Infectious Cholangitis according to the Involved Pathogens

Type of Infectious Cholangitis	Clinical Presentation	Imaging Findings			
		Bile Ducts	Parenchyma	Complications	Treatments
Bacterial cholangitis	Acute, with obstruction	Dilatation, thickened enhanced walls	Edematous areas, contrast enhancement	Portal vein thrombosis, abscesses, secondary sclerosing cholangitis	Antibiotics, drainage
RPC	Recurrent acute episodes	Dilatation, stenosis, intraductal stones, pneumobilia, thickened enhanced walls; left lateral segment usually affected	Atrophy, contrast enhancement	Abscesses, liver failure	Antibiotics, stone removal, dilatation, drainage, partial hepatectomy
Parasites	Silent or subacute, after ingestion of contaminated food or water	Peripheral dilatation without predisposing obstruction, enhancing walls, filling defects (parasites)	<i>E granulosus</i> : cyst <i>E multilocularis</i> : ill-defined infiltration, alveolar cysts <i>C sinensis</i> , <i>O viverrini</i> : none <i>F hepatica</i> : tunnels and caves sign <i>S mansoni</i> , <i>S japonicum</i> : central and peripheral periportal fibrosis and inflammation	RPC, bacterial cholangitis, cholangiocarcinoma	Antiparasites, parasite removal (ERCP); if bacterial superinfection, then treated as for bacterial cholangitis
HIV-related cholangiopathy	Subacute (CD4 count < 100/mm ³)	Intra- and extrahepatic dilatation, stenosis, and pruning; thickened enhancing gallbladder and bile duct walls; sphincter of Oddi stenosis	None	Liver failure	Sphincterotomy; stent placement; sulfamethoxazole and trimethoprim, ganciclovir
Cholangitis lenta	Subacute, after OLT	Intrahepatic dilatation, stenosis, thickened enhancing walls	Parenchymal inflammation	Liver failure	Antibiotics, antifungals, dilatation, new OLT

References

- Boey JH, Way LW. Acute cholangitis. *Ann Surg* 1980;191:264-270.
- Hanau LH, Steigbigel NH. Acute (ascending) cholangitis. *Infect Dis Clin North Am* 2000;14:521-546.
- Kimura Y, Takada T, Kawarada Y, et al. Definitions, pathophysiology, and epidemiology of acute cholangitis and cholecystitis: Tokyo Guidelines. *J Hepatobiliary Pancreat Surg* 2007;14:15-26.
- Csendes A, Diaz JC, Burdiles P, Maluenda F, Morales E. Risk factors and classification of acute suppurative cholangitis. *Br J Surg* 1992;79:655-658.
- Poon RT, Liu CL, Lo CM, et al. Management of gallstone cholangitis in the era of laparoscopic cholecystectomy. *Arch Surg* 2001;136:11-16.
- Tsujino T, Sugita R, Yoshida H, et al. Risk factors for acute suppurative cholangitis caused by bile duct stones. *Eur J Gastroenterol Hepatol* 2007;19:585-588.
- Westphal JF, Brogard JM. Biliary tract infections: a guide to drug treatment. *Drugs* 1999;57:81-91.
- Lee CC, Chang IJ, Lai YC, Chen SY, Chen SC. Epidemiology and prognostic determinants of patients with bacteremic cholecystitis or cholangitis. *Am J Gastroenterol* 2007;102:563-569.
- Qureshi WA. Approach to the patient who has suspected acute bacterial cholangitis. *Gastroenterol Clin North Am* 2006;35:409-423.

10. Rahman SH, Larvin M, McMahon MJ, Thompson D. Clinical presentation and delayed treatment of cholangitis in older people. *Dig Dis Sci* 2005;50:2207–2210.
11. Yu AS, Leung JW. Acute cholangitis. In: Clavien PA, Baillie J, eds. *Diseases of the gallbladder and bile ducts*. Oxford, England: Blackwell, 2001; 205–225.
12. Schulte SJ, Baron RL, Teefey SA, et al. CT of the extrahepatic bile ducts: wall thickness and contrast enhancement in normal and abnormal ducts. *AJR Am J Roentgenol* 1990;154:79–85.
13. Bader TR, Braga L, Beavers KL, Semelka RC. MR imaging findings of infectious cholangitis. *Magn Reson Imaging* 2001;19:781–788.
14. Arai K, Kawai K, Kohda W, Tatsu H, Matsui O, Nakahama T. Dynamic CT of acute cholangitis: early inhomogeneous enhancement of the liver. *AJR Am J Roentgenol* 2003;181:115–118.
15. Lee NK, Kim S, Lee JW, et al. Discrimination of suppurative cholangitis from nonsuppurative cholangitis with computed tomography (CT). *Eur J Radiol* 2009;69:528–535.
16. Yusoff IF, Barkun JS, Barkun AN. Diagnosis and management of cholecystitis and cholangitis. *Gastroenterol Clin North Am* 2003;32:1145–1168.
17. Nagino M, Takada T, Kawarada Y, et al. Methods and timing of biliary drainage for acute cholangitis: Tokyo Guidelines. *J Hepatobiliary Pancreat Surg* 2007;14:68–77.
18. van Erpecum KJ. Complications of bile-duct stones: acute cholangitis and pancreatitis. *Best Pract Res Clin Gastroenterol* 2006;20:1139–1152.
19. Lai EC, Mok FP, Tan ES, et al. Endoscopic biliary drainage for severe acute cholangitis. *N Engl J Med* 1992;326:1582–1586.
20. Bornman PC, van Beljon JI, Krige JE. Management of cholangitis. *J Hepatobiliary Pancreat Surg* 2003;10:406–414.
21. Al-Sukhni W, Gallinger S, Pratzner A, et al. Recurrent pyogenic cholangitis with hepatolithiasis: the role of surgical therapy in North America. *J Gastrointest Surg* 2008;12:496–503.
22. Adson MA, Nagorney DM. Hepatic resection for intrahepatic ductal stones. *Arch Surg* 1982;117:611–616.
23. Heffernan EJ, Geoghegan T, Munk PL, Ho SG, Harris AC. Recurrent pyogenic cholangitis: from imaging to intervention. *AJR Am J Roentgenol* 2009;192:W28–W35.
24. Kim MJ, Cha SW, Mitchell DG, Chung JJ, Park S, Chung JB. MR imaging findings in recurrent pyogenic cholangitis. *AJR Am J Roentgenol* 1999;173:1545–1549.
25. Chan FL, Man SW, Leong LL, Fan ST. Evaluation of recurrent pyogenic cholangitis with CT: analysis of 50 patients. *Radiology* 1989;170:165–169.
26. Kim JH, Kim TK, Eun HW, et al. CT findings of cholangiocarcinoma associated with recurrent pyogenic cholangitis. *AJR Am J Roentgenol* 2006;187:1571–1577.
27. Pitt HA, Venbrux AC, Coleman J, et al. Intrahepatic stones: the transhepatic team approach. *Ann Surg* 1994;219:527–535; discussion 535–537.
28. Czermak BV, Akhan O, Hiemetzberger R, et al. Echinococcosis of the liver. *Abdom Imaging* 2008;33:133–143.
29. McManus DP, Zhang W, Li J, Bartley PB. Echinococcosis. *Lancet* 2003;362:1295–1304.
30. Stamm B, Fejgl M, Hueber C. Satellite cysts and biliary fistulas in hydatid liver disease: a retrospective study of 17 liver resections. *Hum Pathol* 2008;39:231–235.
31. Simsek H, Ozaslan E, Sayek I, et al. Diagnostic and therapeutic ERCP in hepatic hydatid disease. *Gastrointest Endosc* 2003;58:384–389.
32. Mueller PR, Dawson SL, Ferrucci JT Jr, Nardi GL. Hepatic echinococcal cyst: successful percutaneous drainage. *Radiology* 1985;155:627–628.
33. Khuroo MS, Wani NA, Javid G, et al. Percutaneous drainage compared with surgery for hepatic hydatid cysts. *N Engl J Med* 1997;337:881–887.
34. Kodama Y, Fujita N, Shimizu T, et al. Alveolar echinococcosis: MR findings in the liver. *Radiology* 2003;228:172–177.
35. Lim JH, Mairiang E, Ahn GH. Biliary parasitic diseases including clonorchiasis, opisthorchiasis and fascioliasis. *Abdom Imaging* 2008;33:157–165.
36. Chan HH, Lai KH, Lo GH, et al. The clinical and cholangiographic picture of hepatic clonorchiasis. *J Clin Gastroenterol* 2002;34:183–186.
37. Jeong YY, Kang HK, Kim JW, Yoon W, Chung TW, Ko SW. MR imaging findings of clonorchiasis. *Korean J Radiol* 2004;5:25–30.
38. Aksoy DY, Kerimoglu U, Oto A, et al. Infection with *Fasciola hepatica*. *Clin Microbiol Infect* 2005;11:859–861.
39. Arjona R, Riancho JA, Aguado JM, Salesa R, Gonzalez-Macias J. Fascioliasis in developed countries: a review of classic and aberrant forms of the disease. *Medicine (Baltimore)* 1995;74:13–23.
40. Shah OJ, Zargar SA, Robbani I. Biliary ascariasis: a review. *World J Surg* 2006;30:1500–1506.
41. Das CJ, Kumar J, Debnath J, Chaudhry A. Imaging of ascariasis. *Australas Radiol* 2007;51:500–506.
42. Bethony J, Brooker S, Albonico M, et al. Soil-transmitted helminth infections: ascariasis, trichuriasis, and hookworm. *Lancet* 2006;367:1521–1532.
43. Astudillo JA, Sporn E, Serrano B, Astudillo R. Ascariasis in the hepatobiliary system: laparoscopic management. *J Am Coll Surg* 2008;207:527–532.
44. Rocha Mde S, Costa NS, Costa JC, et al. CT identification of *Ascaris* in the biliary tract. *Abdom Imaging* 1995;20:317–319.
45. Ross AG, Bartley PB, Sleight AC, et al. Schistosomiasis. *N Engl J Med* 2002;346:1212–1220.
46. Manzella A, Ohtomo K, Monzawa S, Lim JH. Schistosomiasis of the liver. *Abdom Imaging* 2008;33:144–150.
47. Vianna MR, Gayotto LC, Telma R, et al. Intrahepatic bile duct changes in human hepatosplenic schistosomiasis *mansoni*. *Liver* 1989;9:100–109.
48. Brant PE, Kopke-Aguilar L, Shigueoka DC, et al. Anicteric cholangiopathy in schistosomiasis patients. *Acta Trop* 2008;108:218–221.
49. Bezerra AS, D'Ippolito G, Caldana RP, Cecin AO, Ahmed M, Szejnfeld J. Chronic hepatosplenic schistosomiasis *mansoni*: magnetic resonance imaging and magnetic resonance angiography findings. *Acta Radiol* 2007;48:125–134.
50. Keaveny AP, Karasik MS. Hepatobiliary and pancreatic infections in AIDS: part II. *AIDS Patient Care STDS* 1998;12:451–456.

51. Mahajani RV, Uzer MF. Cholangiopathy in HIV-infected patients. *Clin Liver Dis* 1999;3:669-684.
52. Barthet M, Chauveau E, Bonnet E, et al. Pancreatic ductal changes in HIV-infected patients. *Gastrointest Endosc* 1997;45:59-63.
53. Cello JP. Human immunodeficiency virus-associated biliary tract disease. *Semin Liver Dis* 1992;12:213-218.
54. Bilgin M, Balci NC, Erdogan A, Momtahan AJ, Alkaade S, Rau WS. Hepatobiliary and pancreatic MRI and MRCP findings in patients with HIV infection. *AJR Am J Roentgenol* 2008;191:228-232.
55. Bouche H, Housset C, Dumont JL, et al. AIDS-related cholangitis: diagnostic features and course in 15 patients. *J Hepatol* 1993;17:34-39.
56. Farman J, Brunetti J, Baer JW, et al. AIDS-related cholangiopancreatographic changes. *Abdom Imag* 1994;19:417-422.
57. Rubin R, Munoz SJ, Moritz M. Rejection-independent cholangitis and cirrhosis following orthotopic liver transplantation. *Hum Pathol* 1993;24:996-1002.
58. Lin CC, Sundaram SS, Hart J, Whittington PF. Subacute nonsuppurative cholangitis (cholangitis lenta) in pediatric liver transplant patients. *J Pediatr Gastroenterol Nutr* 2007;45:228-233.
59. Wise PE, Pinson CW. Biliary complications of liver transplantation. In: Clavien PA, Baillie J, eds. *Diseases of the gallbladder and bile ducts*. Oxford, England: Blackwell, 2001; 245-257.
60. Millionig G, Buratti T, Graziadei IW, et al. Bactobilia after liver transplantation: frequency and antibiotic susceptibility. *Liver Transpl* 2006;12:747-753.
61. Wade JJ, Rolando N, Hayllar K, Philpott-Howard J, Casewell MW, Williams R. Bacterial and fungal infections after liver transplantation: an analysis of 284 patients. *Hepatology* 1995;21:1328-1336.
62. Patel R, Badley AD, Larson-Keller J, et al. Relevance and risk factors of enterococcal bacteremia following liver transplantation. *Transplantation* 1996;61:1192-1197.
63. Fulcher AS, Turner MA, Ham JM. Late biliary complications in right lobe living donor transplantation recipients: imaging findings and therapeutic interventions. *J Comput Assist Tomogr* 2002;26:422-427.
64. De Moor V, El Nakadi I, Jeanmart J, Gelin M, Donckier V. Cholangitis caused by Roux-en-Y hepaticojejunostomy obstruction by a biliary stone after liver transplantation. *Transplantation* 2003;75:416-418.
65. Kitazono MT, Qayyum A, Yeh BM, Chard PS, Ostroff JW, Coakley FV. Magnetic resonance cholangiography of biliary strictures after liver transplantation: a prospective double-blind study. *J Magn Reson Imaging* 2007;25:1168-1173.
66. Miraglia R, Maruzzelli L, Caruso S, et al. Percutaneous management of biliary strictures after pediatric liver transplantation. *Cardiovasc Intervent Radiol* 2008;31:993-998.
67. Laor T, Hoffer FA, Vacanti JP, Jonas MM. MR cholangiography in children after liver transplantation from living related donors. *AJR Am J Roentgenol* 1998;170:683-687.
68. Norton KI, Lee JS, Kogan D, et al. The role of magnetic resonance cholangiography in the management of children and young adults after liver transplantation. *Pediatr Transplant* 2001;5:410-418.
69. Pilleul F, Guibaud L, Dugougeat F, Lachaud A, Pracros J. MR cholangiography in biliary complications after liver transplantation in children [in French]. *J Radiol* 2000;81:793-798.
70. Stelzmueller I, Berger N, Wiesmayr S, et al. Group milleri streptococci: significant pathogens in solid organ recipients. *Transpl Int* 2007;20:51-56.
71. Koivusalo A, Isoniemi H, Salmela K, Hockerstedt K. Biliary complications in 100 adult liver transplantations: a retrospective clinical study. *Transpl Int* 1994;7(suppl 1):S119-S120.
72. Oku T, Maeda M, Waga E, et al. Cytomegalovirus cholangitis and pancreatitis in an immunocompetent patient. *J Gastroenterol* 2005;40:987-992.
73. Halme L, Hockerstedt K, Lautenschlager I. Cytomegalovirus infection and development of biliary complications after liver transplantation. *Transplantation* 2003;75:1853-1858.
74. Brundler MA, Rodriguez-Baez N, Jaffe R, Weinberg AG, Rogers BB. Adenovirus ascending cholangiohepatitis. *Pediatr Dev Pathol* 2003;6:156-159.
75. Campos M, Jouzdani E, Sempoux C, et al. Sclerosing cholangitis associated to cryptosporidiosis in liver-transplanted children. *Eur J Pediatr* 2000;159:113-115.
76. Denkinger CM, Harigopal P, Ruiz P, Dowdy LM. Cryptosporidium parvum-associated sclerosing cholangitis in a liver transplant patient. *Transpl Infect Dis* 2008;10:133-136.

Biliary Infections: Spectrum of Imaging Findings and Management

Onofrio A. Catalano, MD, et al

RadioGraphics 2009; 29:2059–2080 • Published online 10.1148/rg.297095051 • Content Codes: **GI** **VI**

Page 2060

Development of BAC requires biliary bacterial contamination, stagnant bile, and increased intrabiliary pressure (≥ 20 cm H₂O) (2–4).

Page 2062

Enhancement of intrahepatic biliary duct walls is a common finding, reported in up to 92% of cases investigated with MR imaging. It is best seen with gadolinium-enhanced delayed phase fat-suppressed sequences (13).

Page 2065

At imaging, RPC is characterized by stenosis or strictures of the peripheral ducts, with decreased **branching and abrupt tapering (“arrowhead appearance”)** associated with **disproportionate dilatation** of the central and extrahepatic bile ducts (Fig 8). Central dilatation tends to be diffuse, involving both stone-bearing and stone-free ducts. The periportal space is thickened owing to periductal inflammation and fibrosis (23,24).

Page 2067

Imaging findings of echinococcosis caused by *E granulosus* reflect the different stages of the hydatid cyst.

Page 2075

Imaging findings resemble those of sclerosing cholangitis but are associated with papillary stenosis and long extrahepatic bile duct strictures. Typical features include intra- and extrahepatic biliary dilatation with predominant left-sided biliary involvement. Other findings include saccular dilatations, debris, pruning, irregular thickening of the CBD, papillary stenosis, and acalculous cholecystitis (Figs 19, 20). The bile duct and gallbladder walls are usually thickened.